https://doi.org/10.5607/en.2017.26.2.71
Exp Neurobiol. 2017 Apr;26(2):71-81.
pISSN 1226-2560 • eISSN 2093-8144

Original Article

Experimental Neurobiology

Check for updates

Flow Shear Stress Enhances the Proliferative Potential of Cultured Radial Glial Cells Possibly Via an Activation of Mechanosensitive Calcium Channel

Min Gu Park[1,2,3†], Heeyeong Jang[5†], Sang-Hoon Lee[1,4,5] and C. Justin Lee[1,2,3*]

[1]KU-KIST Graduate School of Converging Science and Technology, Korea University, Seoul 02841,
[2]Center for Neuroscience and Functional Connectomics, Korea Institute of Science and Technology (KIST), Seoul 02792,
[3]Center for Glia-Neuron Interaction, Korea Institute of Science and Technology (KIST), Seoul 02792,
[4]School of Biomedical Engineering, College of Health Science, Korea University, Seoul 02841,
[5]Department of Bio-convergence Engineering, College of Health Science, Korea University, Seoul 02841, Korea

Radial glial cells (RGCs) which function as neural stem cells are known to be non-excitable and their proliferation depends on the intracellular calcium (Ca^{2+}) level. It has been well established that Inositol 1,4,5-trisphosphate (IP_3)-mediated Ca^{2+} release and Ca^{2+} entry through various Ca^{2+} channels are involved in the proliferation of RGCs. Furthermore, RGCs line the ventricular wall and are exposed to a shear stress due to a physical contact with the cerebrospinal fluid (CSF). However, little is known about how the Ca^{2+} entry through mechanosensitive ion channels affects the proliferation of RGCs. Hence, we hypothesized that shear stress due to a flow of CSF boosts the proliferative potential of RGCs possibly via an activation of mechanosensitive Ca^{2+} channel during the embryonic brain development. Here, we developed a new microfluidic two-dimensional culture system to establish a link between the flow shear stress and the proliferative activity of cultured RGCs. Using this microfluidic device, we successfully visualized the artificial CSF and RGCs in direct contact and found a significant enhancement of proliferative capacity of RGCs in response to increased shear stress. To determine if there are any mechanosensitive ion channels involved, a mechanical stimulation by poking was given to individual RGCs. We found that a poking on radial glial cell induced an increase in intracellular Ca^{2+} level, which disappeared under the extracellular Ca^{2+}-free condition. Our results suggest that the shear stress by CSF flow possibly activates mechanosensitive Ca^{2+} channels, which gives rise to a Ca^{2+} entry which enhances the proliferative capacity of RGCs.

Key words: Radial glial cell, Shear stress, Mechanosensitive ion channel

INTRODUCTION

Neural stem cells (NSCs) are multipotent cells in the central nervous system (CNS). NSCs can self-renew and differentiate into three cell types commonly found in the CNS — neurons, astrocytes, and oligodendrocytes [1]. The dynamic equilibrium between self-renewal and differentiation of NSCs is critical to both the maintenance of the stem cell pool and active neurogenesis during the embryonic brain development [2]. In the beginning

Received March 21, 2017, Revised April 5, 2017,
Accepted April 5, 2017

*To whom correspondence should be addressed.
TEL: 82-2-958-6421, FAX: 82-2-958-6919
e-mail: cjl@kist.re.kr
†These authors contributed equally to this work.

of embryogenesis, the embryonic brain forms an open tube that becomes sequentially sealed anteriorly and posteriorly to establish a ventricular system. The ventricular system rapidly expands by an accumulation of cerebrospinal fluid (CSF) within ventricles, whose borders are lined up with neuroepithelial cells (NEPs), which are considered as embryonic NSCs [3, 4]. As the development proceeds, NEPs progressively convert to radial glial cells (RGCs) which are also recognized as NSCs. Embryonic RGCs play a structural role in guiding neuronal migration, sustain the potential to differentiate into neurons, glial cells, and ependymal cells, and expand through distinct layers of the developing brain [5,6].

RGCs are non-excitable cells whose proliferation is tightly controlled by intracellular calcium (Ca^{2+}) level [7, 8]. Adenosine triphosphate (ATP) signaling has been shown to be involved in proliferation of RGCs, as ATP activates purinergic receptors resulting in inositol 1,4,5-trisphosphate (IP_3)-mediated Ca^{2+} release from endoplasmic reticulum (ER) [9-11]. Another study reported that embryonic stem cell-derived neural progenitors form networks exhibiting synchronous Ca^{2+} activity that stimulates cell proliferation. The Ca^{2+} wave propagates from cell to cell via connexin 43 (Cx43) gap junctions leading to an activation of voltage-dependent Ca^{2+} channels (VGCCs) in the plasma membrane [12]. It has also been well studied that basic fibroblast growth factor (bFGF) induces proliferation of RGCs via Cx43 upregulation [13]. The canonical transient receptor potential 1 (TRPC1) was recently shown to contribute to the bFGF-mediated Ca^{2+} entry, which is involved in self-renewal of embryonic rat NSCs [14]. Finally, the Ca^{2+} signaling has been shown to be critical for the proliferation and regulation of the cell cycle in NSCs, mainly early in G1 and at the G1/S and G2/M transitions [15-18].

Together with chemical and hormonal factors, NSCs encounter many mechanical forces during the embryonic brain development. It has been demonstrated that the tissue folding and cell sheet movements during the CNS development create local physical stress on endogenous NSCs [19, 20]. The fate of NSCs is shown to be strongly influenced by the stiffness of substrate *in vitro* in a range physiologically relevant for CNS tissue [21-24]. In addition, ventricular and subventricular zones show significant shifts in stiffness during the brain development, which is correlated with cell fate determination of NSCs [25]. CSF also creates mechanical forces on NSCs. It has been shown that positive hydrostatic pressure of CSF stimulates the proliferation of NEPs [26]. Additionally, in mammalian lateral ventricles, a pressure gradient arising from CSF secretion in choroid plexus (ChP) (developing from E14 in mice and E15.5 in rats [27]) and CSF absorption in the foramen of Monroe, an opening that connects the left and right sides of the lateral ventricles in the brain, is very likely to initiate CSF flow in the caudo-rostral direction [28]. At this time, the ventricular zone of the embryonic brain is mostly covered with RGCs [29]. As a result, RGCs in the ventricular zone are in physical contact with CSF flow, which causes hydrodynamic forces on the ventricular wall and thus on RGCs. Because these mechanical forces are at play during development, it would be worthwhile to investigate the influence of the hydrodynamic forces by CSF flow on properties of RGCs. Moreover, RGCs have primary cilia which face the ventricular lumen and are thought to receive chemical and mechanical stimuli [30, 31]. Hence, we hypothesized that shear stress due to flow of CSF enhances the proliferation of RGCs potentially via a Ca^{2+} entry through mechanosensitive ion channels.

In this study, we have explored the latest concepts of microfluidics to mimic the in vivo microenvironment experienced by RGCs during the embryonic brain development. The most obvious advantages of microfluidics include small sample volumes, rapid results, and lower costs [32-34]. We have developed a microfluidic 2D culture system to give continuous and uniform shear stress on RGCs. Using this microfluidic device, we successfully visualized and monitored the effects of flow shear stress on the proliferative capacity of RGCs. In order to investigate the existence of mechanosensitive Ca^{2+} channel on RGCs, mechanical stimulation by poking was given to individual RGCs and changes in cytosolic calcium concentration were measured with the Fura-2 ratiometric imaging of Ca^{2+}. We have found that RGCs respond rigorously to mechanical stimulations and shear stress by Ca^{2+} increase and enhanced proliferation, respectively.

MATERIALS AND METHODS

Fabrication of microfluidic chip

The microfluidic chip made of PDMS was fabricated by photolithography and replica molding using photoresist patterns as master templates. SU-8, a negative photoresist on a silicon wafer, was patterned by photolithography, and 50 μm deep main channels were generated. After the photolithography process, the photoresist pattern was developed and washed to clear debris. Well-mixed PDMS prepolymer and curing agent (Sylgard184; Dow Corning, Midland, MI, USA) were poured onto the master template and cured in an oven at 120°C for 1 hour. The PDMS plate was then peeled from the master template, and an inlet and an outlet were punched with a sharp needle. The surfaces of the PDMS plate and slide glass were oxidized by O2 plasma using a plasma reactor. After binding the PDMS piece to the slide glass, the device was kept at 90°C for 1 h to allow complete annealing. Syringe pump and the inlet of the chip were connected by flexible polytetrafluoroethylene (PTFE) tubing (inner diameter, 1.0 mm; outer diameter, 1.5

https://doi.org/10.5607/en.2017.26.2.71

mm). The outlet of the chip was connected to a reservoir by PTFE tubing.

Computational evaluation of wall shear stress

We computationally simulated the wall shear stress distribution in the channel to identify the region of the flow channel in which a uniform shear stress level could be expected. Three-dimensional flow in the microfluidic channel was modeled using a finite volume method with microfluidics module of COMSOL Multiphysics 4.3 (Stockholm, Sweden) (Fig. 1c). A structured grid system was created to model the main region of the channel for high computing performance. The steady-state Navier–Stokes equations were solved to analyze the flow field. The working fluid was assumed to be a homogeneous, incompressible Newtonian fluid. The physical properties of the culture medium was as follows; density is 993.2 kg/m3 (same as water), dynamic viscosity is 0.000785 kg/m·s (1.04 times that of water) at 37°C [35]. The boundary conditions consisted of a constant flow rate at the inlet and atmospheric pressure at the outlet. The no-slip boundary condition was assumed for other surfaces. The shear stress generated in the main channel was directly dependent on the velocity profile, because the flow could be modeled as Poiseuille flow in our microchip. For accurate prediction of WSS in the calculation, an appropriate grid density near the wall (channel bottom) was very important. Because wall shear stress was calculated as the first derivative of the flow velocity near the wall, an appropriate grid density near the wall was essential to accurately follow the velocity profile. Therefore, special care was given to the wall shear stress evaluation due to its strong dependency on the vertical grid density (Fig. 1c, inset). To quantify the detailed local distribution of shear stress, stress was computed along two orthogonal lines (A–B and X–Y in Fig. 1b). The results showed a flat shear stress profile everywhere within uniform shear region (Fig. 1b). Therefore, the cells were exposed to a uniform shear stress in a given observation region. Shear stress was calculated at 10 μm above the bottom of the channel, allowing for the height of the cell.

Cell culture

Primary cortical NSCs were isolated from cerebral cortical regions of embryonic day 16 rat embryos (Sprague-Dawley, Koatech, South Korea) using a surgical procedure as previously described [36] and authorized by the Institutional Animal Care and Use Committee (IACUC) of Korea University. NSCs were maintained in DMEM/F12 (Gibco) supplemented with B-27 Supplement w/o vitamin A (Gibco), Penicillin-Streptomycin-Glutamine (Gibco), BSA 7.5% (Gibco), N2 supplement (Gibco), epidermal growth factor (EGF) (Peprotech) and basic fibroblast growth factor (bFGF) (Peprotech). The chip was coated overnight by filling the channels with a solution of laminin (5 μg/ml, Sigma), followed by being coated with a solution of poly-D-lysine (10 μg/ml, Sigma) and washed with PBS before seeding cells. This surface treatment induces neural cell adhesion. A NSC suspension (200 μl of 5.7×10^4 cells/ml) was loaded into the inlet of the chip using a micropipette tip. The cells in the suspension medium sank, attached to the bottom of the channels, and stabilized by being left undisturbed for about 2 hours, after which a constant flow of the medium from the inlet to the outlet was applied to wash out the untrapped cells. Finally, NSCs were cultured for 5 days under different shear stresses. For the Ca^{2+} imaging experiments we identified morphologically for the cells that are elongated and bipolar-shaped as RGCs.

Fixation and immunocytochemistry

Cultured RGCs were fixed with 4% paraformaldehyde (PFA) for 20 min at 4°C and then washed with 0.1% bovine serum albumin diluted in phosphate-buffered saline (PBSA). The cells were treated with 0.1% Triton X-100 diluted in phosphate-buffered saline for 20 min at room temperature and then washed with 0.1% PBSA. The cells were blocked with 3% PBSA for 30 min at room temperature to reduce non-specific protein adsorption and washed with 0.1% PBSA. Afterwards, the cells were incubated overnight at 4°C with primary antibodies: mouse anti-Nestin (1:500 diluted in 1% PBSA, Abcam). Cells were rinsed with 0.1% PBSA and incubated with Alexa Fluor 488-conjugated secondary antibody (1:1000 diluted in 1% PBSA, Invitrogen) for 90 min at room temperature. Fluorescence images were taken using a confocal laser-scanning microscope (Olympus, Japan) after counterstaining the cell nuclei with 4′, 6-diamidino-2-phenylindole dihydrochloride (DAPI) (1:1000 diluted in 1% PBSA, Invitrogen).

Ca^{2+} imaging

For imaging, cultured RGCs were plated as a monolayer on 12-mm glass coverslips coated with poly-D-lysine (Sigma). Astrocytes were incubated with 5 μM Fura-2 AM plus 1 μM pluronic acid (Molecular Probes) for 30 min at room temperature. External solution contained 150 mM NaCl, 10 mM HEPES, 3 mM KCl, 2 mM CaCl2, 1 mM MgCl2, 22 mM sucrose, and 10 mM glucose (pH adjusted to 7.4 and osmolarity to 325 mOsm). Intensity images of 510 nm wavelength were taken at 340 nm and 380 nm excitation wavelengths using iXon EMCCD (DV887 DCS-BV, ANDOR technology, UK). Imaging Workbench version 6.0 (Indec System, CA, USA) was used for acquisition of intensity images and conversion to ratios as previously described [37].

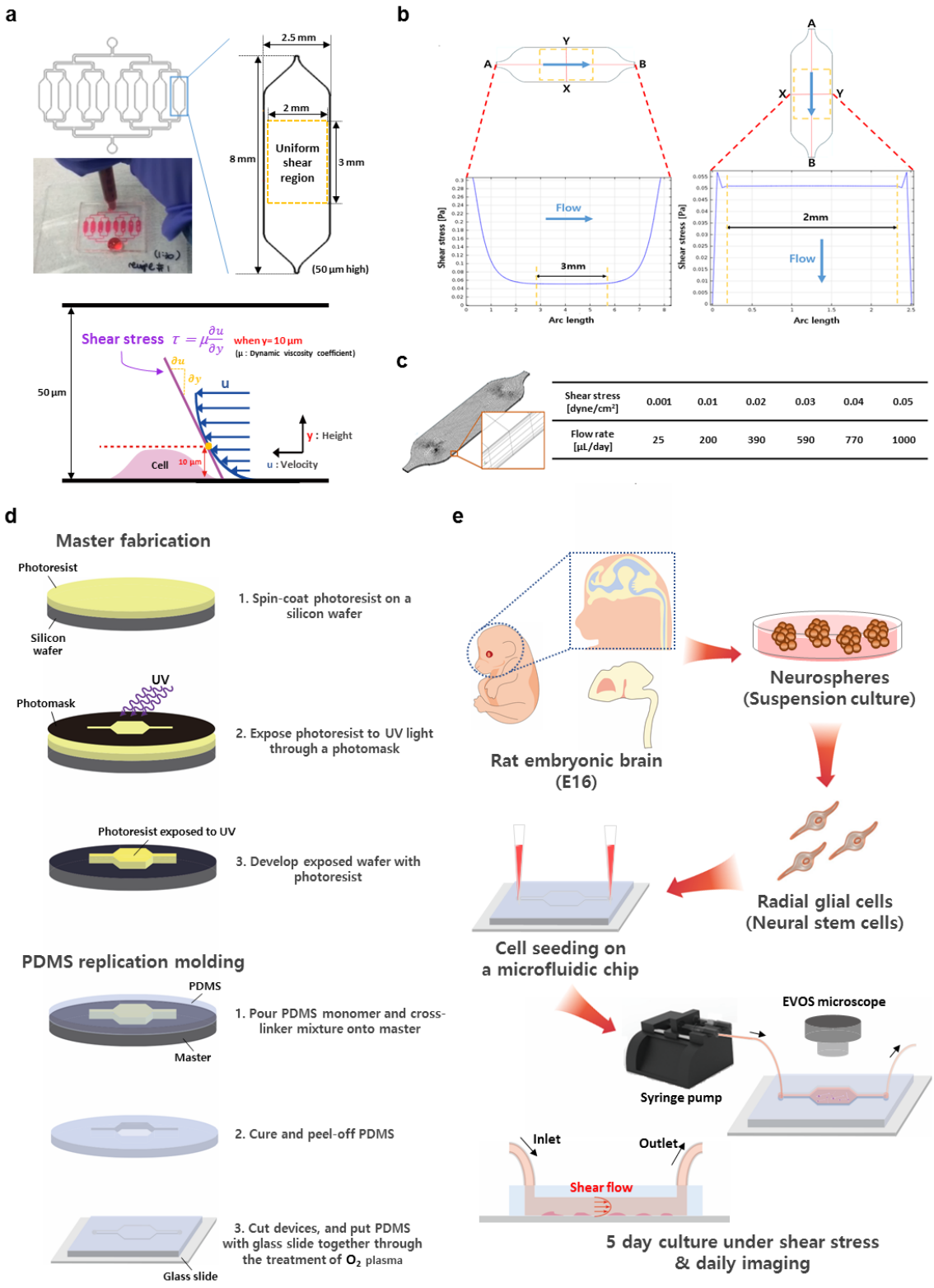

Fig. 1. Microfluidic chip design, fabrication, computational simulation, and operation. (a) Top-view layout of the microfluidic chip with the 8 parallel channels (top) and the principles of the estimation of wall shear stress applied to RGCs (bottom). (b) Detailed wall shear stress profiles at the cross section (A–B) and at the cross section (X–Y). Uniform shear region of the channel, 3 mm-long and 2 mm-wide, shows a uniform wall shear stress (0.05 Pa when flow rate is 6.7 μL/min). (c) The inset of computational geometry with the generated mesh showing a close-up view of the features of the vertical mesh (left) and the table showing relationship between flow rates and corresponding shear stresses (right). (d) Fabrication methods for microfluidic chips. (e) Operational diagram of the microfluidic system for the study of shear stress.

https://doi.org/10.5607/en.2017.26.2.71

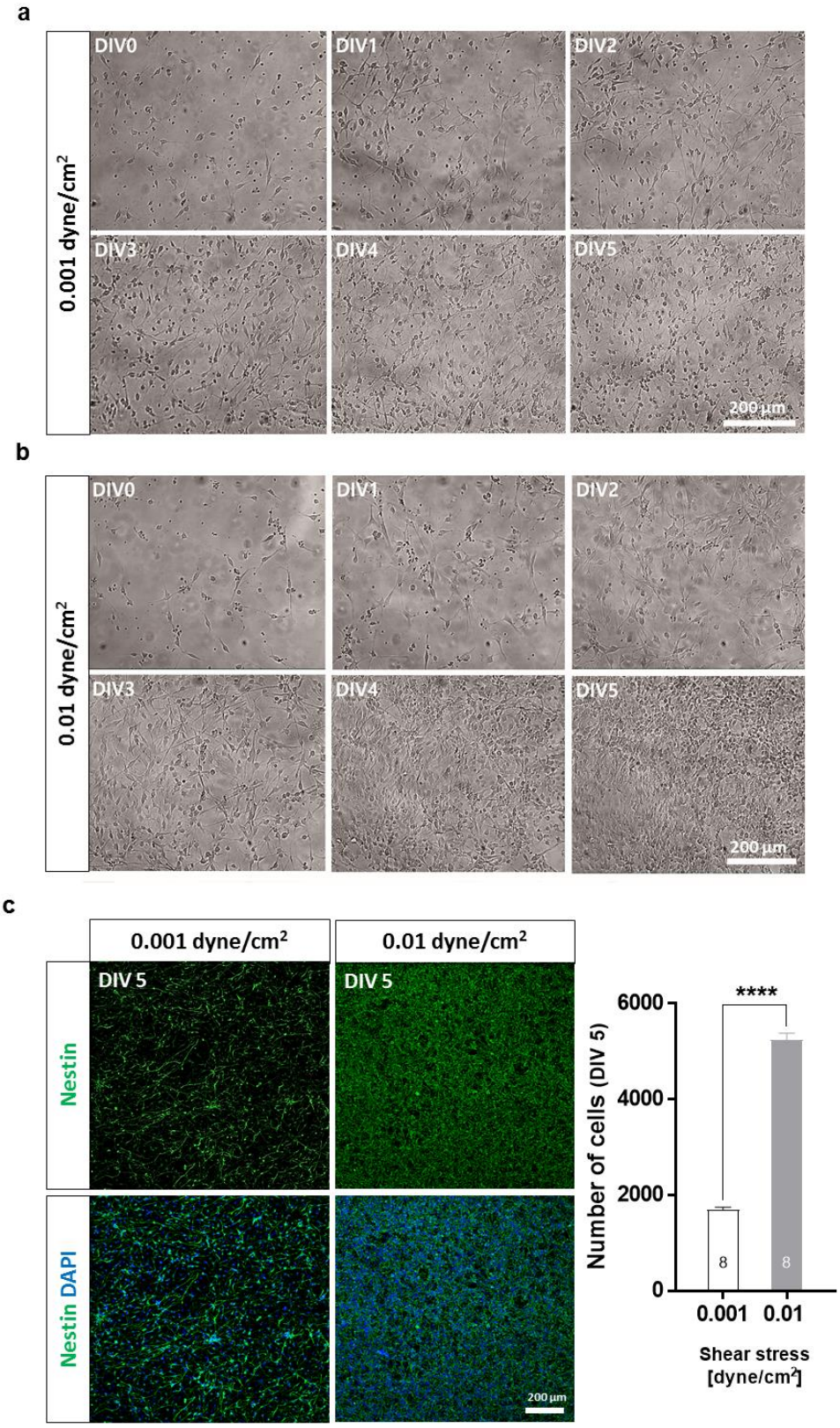

Fig. 2. The effect of physiologically relevant shear stress on the proliferative potential of RGCs. (a) Daily bright-field images of RGCs under 0.001 dyne/cm^2 shear stress for 5 days *in vitro*. (b) Daily bright-field images of RGCs under 0.01 dyne/cm^2 physiologically relevant shear stress for 5 days *in vitro*. (c) Immunofluorescence images of RGCs on DIV5 stained against nestin (green) and DAPI (blue) (left) and summary bar graph showing the comparison of the proliferated cell number on DIV5 (right). Unpaired two-tailed t-test (****p<0.0001).

Data analysis and statistics

To quantify the cell number inside the main channel (Fig. 2c), the DAPI staining images were further analyzed by the image analysis software ImageJ.

For measurements of peak amplitude of Ca^{2+} signal, each 10 seconds of data right before the mechanical stimulation were averaged and subsequently used as a reference baseline from which changes were measured. Search region was set to find the maximum value of Ca^{2+} signal and peak amplitude was calculated using Clampfit 10.4 (Axon Instruments, USA).

All quantitative data were expressed as means±standard error of the mean. D'Agostino & Pearson normality test was performed to judge if data are normally distributed or not. Statistical differences were determined by two-tailed, unpaired t-test with Welch's correction since our data are normally distributed but the variances are unequal.

RESULTS

Uniformly distributed shear stress in a novel microfluidic chip

To mimic the physiologically relevant dynamic shear stress experienced by RGCs in ventricular zone, we fabricated a novel microfluidic chip. Fig. 1a illustrates the chip design concept. The chip contains 8 identical main channels for high throughput experiments. And each main channel is 2.5 mm in width, 8 mm in length, and 0.05 mm in height. The aspect ratio, the proportional relationship between the width and height of the channel, is large enough to give uniform shear stress distribution throughout a large area of the middle region of the channel termed uniform shear region. The wall shear stress (τ) on the cell surface was estimated from $\tau \approx \mu(\partial u/\partial y)$ at y=10 μm, where μ is the dynamic viscosity of the fluid, u is the axial velocity, and y is the height (Fig. 1a). As predicted in the simulations, only the cells in uniform shear region were assumed to be exposed to the same level of shear stress (Fig. 1b). And desired levels of shear stress over RGCs can be induced by applying corresponding flow rates (Fig. 1c). The microfluidic chip made of PDMS was fabricated by photolithography and replica molding using photoresist patterns as master templates (Fig. 1d). RGCs were seeded into the microfluidic chip and continuous, *in vivo*-mimicking shear stress powered by a syringe pump was applied on RGCs (Fig. 1e).

Shear stress enhances the proliferative potential of RGCs

To study the effect of shear stress on the proliferative potential of RGCs, we applied an *in vivo*-mimicking shear stress (0.01 dyne/cm^2) continuously over RGCs in culture for 5 days. The estimated physiological ventricular wall shear stress of CSF *in vivo* (>Postnatal day 20 in mouse) is in the range of 0.01~0.018 dyne/cm^2 [28]. We also prepared cultures of RGCs under extremely low shear stress (0.001 dyne/cm^2) as a control condition, instead of those under static condition to avoid depletion of nutrient, oxygen, and soluble factors. Fig. 2a shows the daily bright-field images of RGCs exposed to 0.001 dyne/cm^2 shear stress for 5 days. Under 0.001 dyne/cm^2 shear stress condition, the number of cells did not change dramatically over 5 days. However, the number of RGCs cultured under 0.01 dyne/cm^2 shear stress was dramatically increased (Fig. 2b).

To accurately quantify the number of proliferated cells and to identify the type of cells, we immunostained the cultures of RGCs against neural stem cell marker, nestin, and nuclear marker, DAPI. The intensity of nestin and DAPI immunostaining was significantly higher in the cultures under 0.01 dyne/cm^2 compared to 0.001 dyne/cm^2 (Fig. 2c). The number of DAPI-positive cells on DIV5 was counted and there was a significant difference between 0.001 dyne/cm^2 and 0.01 dyne/cm^2 (Number of cells (DIV5), 0.001 dyne/cm^2: 1691±58.52, n=8 chips; 0.01 dyne/cm^2: 5244±140.8, n=8 chips) (Fig. 2c). These results indicated that the increase in the number of cells was a direct consequence of enhanced proliferation, suggesting that flow shear stress is one of the critical factors for enhancing RGC proliferation.

Functional mechanosensitive Ca^{2+} channels are expressed in RGCs

The most well-known biosensor for flow shear stress is a mechanosensitive channel. To study if RGCs have mechanosensitive Ca^{2+} channels, we gave mechanical stimulation on RGCs using glass pipette while performing Fura-2 Ca^{2+} imaging. We identified the cells with elongated and bipolar processes as RGCs as shown in insets of Fig. 3a. A glass pipette was placed above a cultured single RGC and lowered slowly while the pipette resistance (R_t) was continuously monitored to determine when the pipette touched the cell membrane as previously described [38]. Once the Fura-2 signal started to change, the pipette was immediately withdrawn from the cell membrane [38]. Poking was given until the change in pipette resistance (ΔR_t) reached about 0.5~1.5 MΩ (Fig. 3a). Fig. 3b shows the representative Fura-2 intensity images before and after mechanical stimulation on a cultured RGC reflecting the increase of Ca^{2+} signals in cytoplasm of RGC evoked by poking (Fig. 3b). Some RGCs were responsive to mechanical stimulation (n=27 out of 48 single cells), while other cells showed no Ca^{2+} response to mechanical stimulation (n=21 out of 48 single cells) (Fig. 3c). To determine the source of mechanically-induced Ca^{2+} increases, we tested whether Ca^{2+} increases by mechanical stimulation can be

https://doi.org/10.5607/en.2017.26.2.71

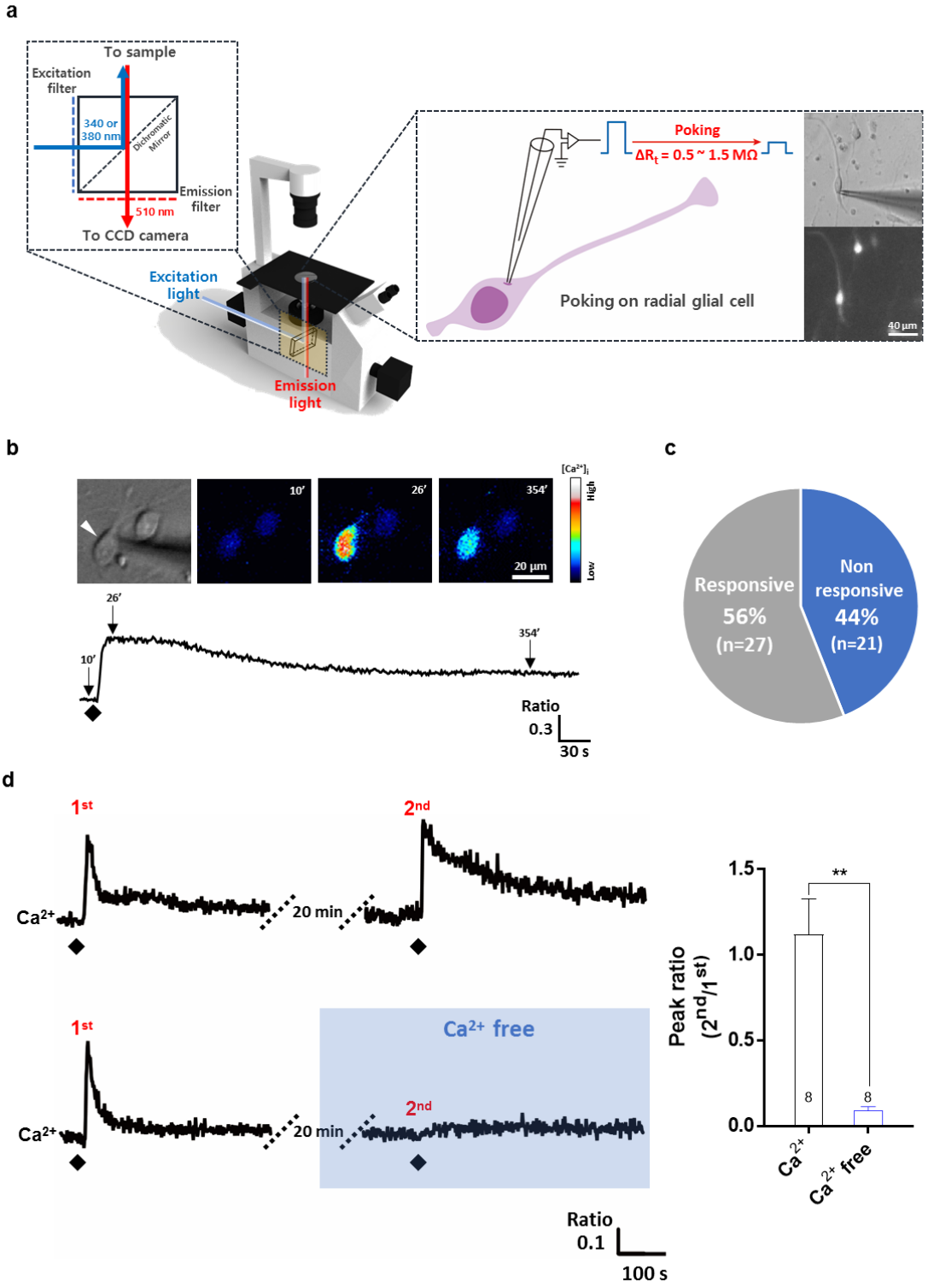

Fig. 3. An activation of mechanosensitive Ca^{2+} channels and subsequent Ca^{2+} entry induced by direct mechanical poking. (a) Schematic illustration of astrocyte Ca^{2+} imaging in inverted microscope using ratiometric Ca^{2+} dye, Fura-2 AM (left). The inset showing representative bright-field image (top right) and Fura-2 AM image (bottom right) of an RGC. (b) The representative bright field image of an RGC and 340/380 ratio images of Ca^{2+} imaging taken at 10 s, 26 s, and 354 s (top). Representative 340/380 ratio trace of poked RGC (bottom). (c) Pie chart showing that the RGCs responsive to poking account for 56% (n=27 out of 48 single cells) and non-responsive RGCs account for 44 % (n=21 out of 48 single cells). (d) Representative 340/380 traces in which two sequential peaks were induced by two sequential poking with 20 min interval (top left) and the 2^{nd} peak was significantly decreased under extracellular Ca^{2+}-free condition (bottom left). Summary bar graph showing $2^{nd}/1^{st}$ peak ratio of 340/380 trace of Ca^{2+} response with and without Ca^{2+} in external solution (right). Unpaired two-tailed t-test (**p<0.01). Diamond indicates the timing of mechanical stimulation.

measured under extracellular Ca^{2+}-free condition. Under normal condition, Ca^{2+} increases were evoked by two sequential mechanical stimulations separated by at least a 20 minute break (Peak ratio ($2^{nd}/1^{st}$), 1.12±0.2082, n=8 cells). However, under extracellular Ca^{2+}-free condition, Ca^{2+} increases evoked by 2^{nd} poking almost completely disappeared (Peak ratio ($2^{nd}/1^{st}$), 0.09025±0.02227, n=8 cells) (Fig. 3d). These results suggest that RGCs have mechanosensitive Ca^{2+} channels which give rise to a Ca^{2+} entry evoked by a mechanical stimulation.

DISCUSSION

In this study, we have investigated the effect of flow shear stress or hydrodynamic pressure on the proliferation of RGCs and mechanically induced-Ca^{2+} entry through mechanosensitive Ca^{2+}-permeable channel on RGCs. We firstly designed the microfluidic chip which provides continuous, uniform and physiologically relevant shear stress on RGCs (Fig. 1). Then we applied a moderate shear stress on RGCs for 5 days and found a significant increase in the number of cells (Fig. 2). Finally, we demonstrated that the Ca^{2+} entry evoked by mechanical stimulation is mediated by mechanosensitive Ca^{2+} channels in RGCs (Fig. 3).

To our knowledge, this is the first investigation of the relationship between CSF-induced shear stress and the proliferation of RGCs by using microfluidics. The fabricated microfluidic chip provided a wide region with uniform shear stress. This allowed us to easily observe the changes in cellular characteristics for a long period of time. The design of the chip was very effective in generating a desired shear stress with a minimal volume of the culture medium: the height of the channel was 50 μm and the total volume of one channel was only about 1 μl (Fig. 1a). However, the cultured RGCs in the microfluidic chip lost their apical-basal polarity when they were plated onto a glass slide. Therefore, unlike the RGCs which experience the shear stress only at the apical surface *in vivo* (Fig. 4a), the cultured RGCs *in vitro* experience the shear stress throughout the entire cell membrane. Nevertheless, our results

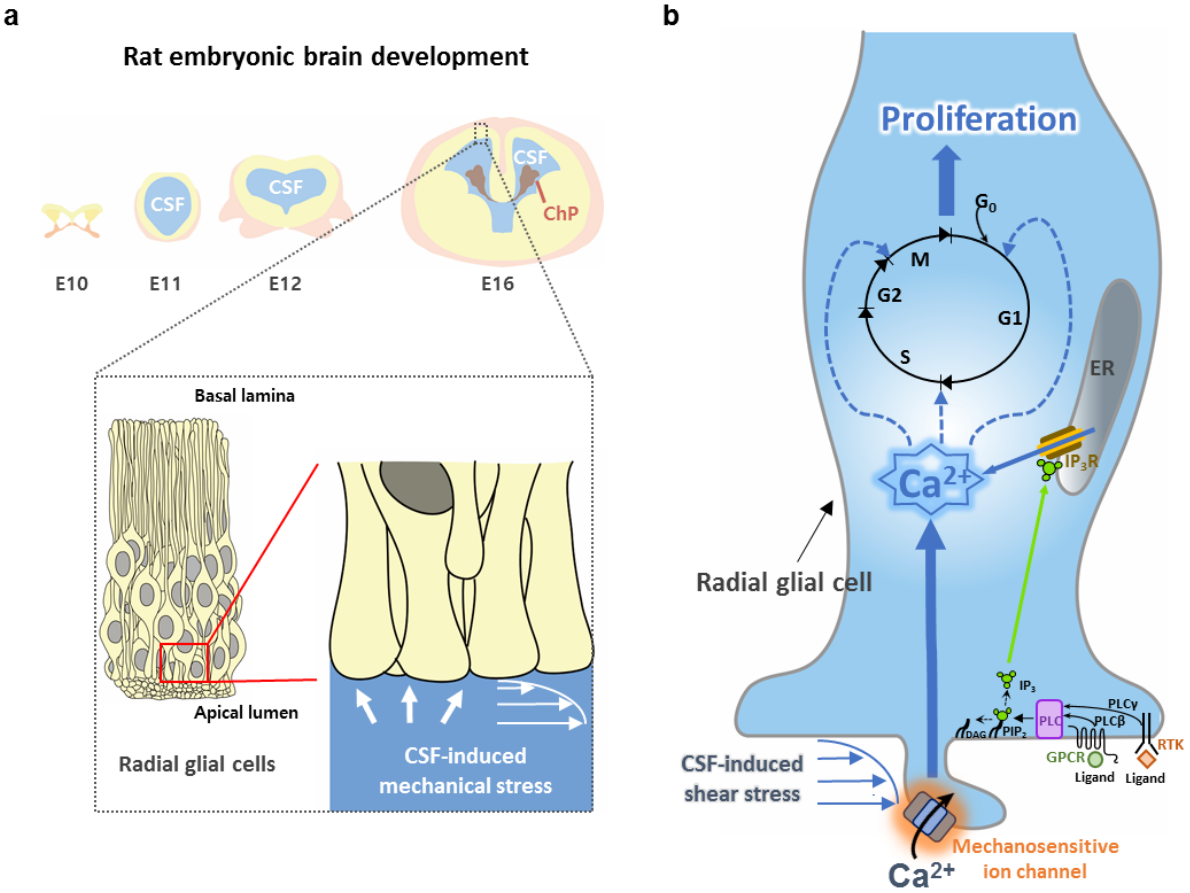

Fig. 4. A novel relationship between RGCs and CSF-induced hydrodynamic pressure during the embryonic brain development. (a) Schematic illustration of rat embryonic brain development. The inset shows the RGCs in ventricular zone experiencing CSF-induced mechanical stress. (b) Schematic diagram of proliferation pathway of RGC initiated by shear stress-induced Ca^{2+} entry.

https://doi.org/10.5607/en.2017.26.2.71

strongly suggest that the CSF-induced shear stress stimulate RGCs at the apical surface of ventricular zone and exert pro-proliferative effects on RGCs. We propose that this happens possibly via an activation of a mechanosensitive Ca^{2+} channels in RGCs (Fig. 4b).

In Fig. 2c, 56% of RGCs were responsive to poking while the rest were not (44%). This could be due to the heterogeneity of RGCs. This is consistent with the previous report that radial glial cells are a heterogeneous population of precursor cells, consisting mainly of neuronal and astroglial precursor cells, and only few multipotential precursor cells [39]. Future studies are needed to further characterize the RGCs in our culture system.

Ca^{2+} signaling of NSCs is considered as the major contributor to proliferation. And we have focused on mechanosensitive Ca^{2+}-permeable channels expressed on NSCs during development. It has been previously reported that spontaneous Ca^{2+} transients in human NEPs require a Ca^{2+} entry from the extracellular environment and the percentage of the cells displaying Ca^{2+} transients was significantly decreased by gadolinium (Gd^{3+}) which is a general inhibitor of transient receptor potential (TRP) channels that are presumably mechanosensitive and non-selective cation channels, whereas application of Ruthenium Red (TRPV family inhibitor) or SKF96365 (TRPC family inhibitor) had no significant effect on spontaneous Ca^{2+} transients [40]. Furthermore, it has been shown that general inhibition of TRP channels by Gd^{3+} significantly attenuated proliferation in human NEPs, whereas TRPC1 shRNA or TRPC4 shRNA as well as Ruthenium Red or SKF96365 did not affect proliferation in the same cells [40], suggesting that other TRP channel family members (other than TRPV or TRPC) might be responsible for Ca^{2+} entry by mechanical stimulation and proliferation of neural stem cells. Recently, TRPA1 was shown to be expressed at a higher level than TRPV1 and TRPV3 in almost all stages in both the choroid plexus and ventricular lining epithelium of developing rat brain [41]. Therefore, it will be interesting to test the possible role of TRPA1 in proliferation of RGCs in the future studies.

Since direct mechanical poking has been used widely to mimic the effect of the shear stress [42, 43], we assumed that shear stress and membrane stretch by poking would possibly activate the same channel. However, further studies are necessary to validate this assumption because it is still not clear whether shear stress and membrane stretch activate the same or different channels [44, 45]. A previous study reported that mechanical stimulation applied in marginal zone of acute coronal brain slices initiates a rapid Ca^{2+} influx from the extracellular space and subsequent Ca^{2+} waves propagate robustly through the ventricular zone [10]. Our results are in line with the previous reports in that mechanical stimulation-induced Ca^{2+} entry occurs in RGCs. These lines of evidence mentioned above raise the possibility that mechanical stimulation could activate Ca^{2+} waves in ventricular zone possibly through an activation of TRP family. It will be of great interest to identify the channel which mediates Ca^{2+} entry induced by mechanical stimulation in future studies. This mechanosensitive channel is most likely the channel mediating the Ca^{2+} entry upon flow shear stress in RGCs.

In summary, we have demonstrated that flow shear stress is a newly found factor which contributes to the enhancement of proliferative potential of RGCs. It is possible that RGCs express mechanically activated-Ca^{2+} channel which is associated with sensing of flow shear stress, leading to proliferation of RGCs. Future investigations will be needed to address these exciting possibilities.

ACKNOWLEDGEMENTS

This study was supported by the KU-KIST School Project, intelligent Bio MEMS Lab (iBML) at Korea University, Creative Research Initiative Program, Korean National Research Foundation (2015R1A3A2066619), and KIST Institutional Grant (2E26662). This paper is dedicated to the late professor Sang-Hoon Lee.

REFERENCES

1. Gage FH (2000) Mammalian neural stem cells. Science 287: 1433-1438.
2. De Filippis L, Binda E (2012) Concise review: self-renewal in the central nervous system: neural stem cells from embryo to adult. Stem Cells Transl Med 1:298-308.
3. Chau KF, Springel MW, Broadbelt KG, Park HY, Topal S, Lun MP, Mullan H, Maynard T, Steen H, LaMantia AS, Lehtinen MK (2015) Progressive differentiation and instructive capacities of amniotic fluid and cerebrospinal fluid proteomes following neural tube closure. Dev Cell 35:789-802.
4. Gato A, Desmond ME (2009) Why the embryo still matters: CSF and the neuroepithelium as interdependent regulators of embryonic brain growth, morphogenesis and histiogenesis. Dev Biol 327:263-272.
5. Markó K, Kohidi T, Hádinger N, Jelitai M, Mezo G, Madarász E (2011) Isolation of radial glia-like neural stem cells from fetal and adult mouse forebrain via selective adhesion to a novel adhesive peptide-conjugate. PLoS One 6:e28538.
6. Malatesta P, Götz M (2013) Radial glia - from boring cables to stem cell stars. Development 140:483-486.
7. Lecca D, Fumagalli M, Ceruti S, Abbracchio MP (2016) Intertwining extracellular nucleotides and their receptors with Ca2+ in determining adult neural stem cell survival, pro-

liferation and final fate. Philos Trans R Soc Lond B Biol Sci 371:20150433.
8. García-García E, Pino-Barrio MJ, López-Medina L, Martínez-Serrano A (2012) Intermediate progenitors are increased by lengthening of the cell cycle through calcium signaling and p53 expression in human neural progenitors. Mol Biol Cell 23:1167-1180.
9. Scemes E, Duval N, Meda P (2003) Reduced expression of P2Y1 receptors in connexin43-null mice alters calcium signaling and migration of neural progenitor cells. J Neurosci 23:11444-11452.
10. Weissman TA, Riquelme PA, Ivic L, Flint AC, Kriegstein AR (2004) Calcium waves propagate through radial glial cells and modulate proliferation in the developing neocortex. Neuron 43:647-661.
11. Pearson RA, Dale N, Llaudet E, Mobbs P (2005) ATP released via gap junction hemichannels from the pigment epithelium regulates neural retinal progenitor proliferation. Neuron 46:731-744.
12. Malmersjö S, Rebellato P, Smedler E, Planert H, Kanatani S, Liste I, Nanou E, Sunner H, Abdelhady S, Zhang S, Andäng M, El Manira A, Silberberg G, Arenas E, Uhlén P (2013) Neural progenitors organize in small-world networks to promote cell proliferation. Proc Natl Acad Sci U S A 110:E1524-E1532.
13. Nadarajah B, Makarenkova H, Becker DL, Evans WH, Parnavelas JG (1998) Basic FGF increases communication between cells of the developing neocortex. J Neurosci 18:7881-7890.
14. Fiorio Pla A, Maric D, Brazer SC, Giacobini P, Liu X, Chang YH, Ambudkar IS, Barker JL (2005) Canonical transient receptor potential 1 plays a role in basic fibroblast growth factor (bFGF)/FGF receptor-1-induced Ca2+ entry and embryonic rat neural stem cell proliferation. J Neurosci 25:2687-2701.
15. Takahashi T, Nowakowski RS, Caviness VS Jr (1995) The cell cycle of the pseudostratified ventricular epithelium of the embryonic murine cerebral wall. J Neurosci 15:6046-6057.
16. Lange C, Huttner WB, Calegari F (2009) Cdk4/cyclinD1 overexpression in neural stem cells shortens G1, delays neurogenesis, and promotes the generation and expansion of basal progenitors. Cell Stem Cell 5:320-331.
17. Salomoni P, Calegari F (2010) Cell cycle control of mammalian neural stem cells: putting a speed limit on G1. Trends Cell Biol 20:233-243.
18. Pauklin S, Vallier L (2013) The cell-cycle state of stem cells determines cell fate propensity. Cell 155:135-147.
19. Nishimura T, Honda H, Takeichi M (2012) Planar cell polarity links axes of spatial dynamics in neural-tube closure. Cell 149:1084-1097.
20. Suzuki M, Morita H, Ueno N (2012) Molecular mechanisms of cell shape changes that contribute to vertebrate neural tube closure. Dev Growth Differ 54:266-276.
21. Tyler WJ (2012) The mechanobiology of brain function. Nat Rev Neurosci 13:867-878.
22. Saha K, Keung AJ, Irwin EF, Li Y, Little L, Schaffer DV, Healy KE (2008) Substrate modulus directs neural stem cell behavior. Biophys J 95:4426-4438.
23. Leipzig ND, Shoichet MS (2009) The effect of substrate stiffness on adult neural stem cell behavior. Biomaterials 30:6867-6878.
24. Keung AJ, de Juan-Pardo EM, Schaffer DV, Kumar S (2011) Rho GTPases mediate the mechanosensitive lineage commitment of neural stem cells. Stem Cells 29:1886-1897.
25. Iwashita M, Kataoka N, Toida K, Kosodo Y (2014) Systematic profiling of spatiotemporal tissue and cellular stiffness in the developing brain. Development 141:3793-3798.
26. Desmond ME, Knepper JE, DiBenedetto AJ, Malaugh E, Callejo S, Carretero R, Alonso MI, Gato A (2014) Focal adhesion kinase as a mechanotransducer during rapid brain growth of the chick embryo. Int J Dev Biol 58:35-43.
27. Val P, Lefrançois-Martinez AM, Veyssière G, Martinez A (2003) SF-1 a key player in the development and differentiation of steroidogenic tissues. Nucl Recept 1:8.
28. Guirao B, Meunier A, Mortaud S, Aguilar A, Corsi JM, Strehl L, Hirota Y, Desoeuvre A, Boutin C, Han YG, Mirzadeh Z, Cremer H, Montcouquiol M, Sawamoto K, Spassky N (2010) Coupling between hydrodynamic forces and planar cell polarity orients mammalian motile cilia. Nat Cell Biol 12:341-350.
29. Mori T, Buffo A, Götz M (2005) The novel roles of glial cells revisited: the contribution of radial glia and astrocytes to neurogenesis. Curr Top Dev Biol 69:67-99.
30. Delling M, DeCaen PG, Doerner JF, Febvay S, Clapham DE (2013) Primary cilia are specialized calcium signalling organelles. Nature 504:311-314.
31. Tong CK, Han YG, Shah JK, Obernier K, Guinto CD, Alvarez-Buylla A (2014) Primary cilia are required in a unique subpopulation of neural progenitors. Proc Natl Acad Sci U S A 111:12438-12443.
32. Pihl J, Karlsson M, Chiu DT (2005) Microfluidic technologies in drug discovery. Drug Discov Today 10:1377-1383.
33. Whitesides GM (2006) The origins and the future of microfluidics. Nature 442:368-373.
34. Pihl J, Sinclair J, Karlsson M, Orwar O (2005) Microfluidics for cell-based assays. Mater Today 8:46-51.
35. Park JY, Yoo SJ, Patel L, Lee SH, Lee SH (2010) Cell morpho-

logical response to low shear stress in a two-dimensional culture microsystem with magnitudes comparable to interstitial shear stress. Biorheology 47:165-178.
36. Park J, Lee BK, Jeong GS, Hyun JK, Lee CJ, Lee SH (2015) Three-dimensional brain-on-a-chip with an interstitial level of flow and its application as an in vitro model of Alzheimer's disease. Lab Chip 15:141-150.
37. Kang SS, Han KS, Ku BM, Lee YK, Hong J, Shin HY, Almonte AG, Woo DH, Brat DJ, Hwang EM, Yoo SH, Chung CK, Park SH, Paek SH, Roh EJ, Lee SJ, Park JY, Traynelis SF, Lee CJ (2010) Caffeine-mediated inhibition of calcium release channel inositol 1,4,5-trisphosphate receptor subtype 3 blocks glioblastoma invasion and extends survival. Cancer Res 70:1173-1183.
38. Lee J, Chun YE, Han KS, Lee J, Woo DH, Lee CJ (2015) Ca(2+) entry is required for mechanical stimulation-induced ATP release from astrocyte. Exp Neurobiol 24:17-23.
39. Malatesta P, Hartfuss E, Götz M (2000) Isolation of radial glial cells by fluorescent-activated cell sorting reveals a neuronal lineage. Development 127:5253-5263.
40. Weick JP, Austin Johnson M, Zhang SC (2009) Developmental regulation of human embryonic stem cell-derived neurons by calcium entry via transient receptor potential channels. Stem Cells 27:2906-2916.
41. Jo KD, Lee KS, Lee WT, Hur MS, Kim HJ (2013) Expression of transient receptor potential channels in the ependymal cells of the developing rat brain. Anat Cell Biol 46:68-78.
42. Verkhovsky AB, Svitkina TM, Borisy GG (1999) Self-polarization and directional motility of cytoplasm. Curr Biol 9:11-20.
43. Sigurdson WJ, Sachs F, Diamond SL (1993) Mechanical perturbation of cultured human endothelial cells causes rapid increases of intracellular calcium. Am J Physiol 264:H1745-H1752.
44. Tykocki T, Kornakiewicz A, Acewicz A, Kostkiewicz B (2015) The role of transient receptor potential channels in the pathogenesis of cerebral aneurysm formation. Asian J Neurosurg 2:1031.
45. Hill-Eubanks DC, Gonzales AL, Sonkusare SK, Nelson MT (2014) Vascular TRP channels: performing under pressure and going with the flow. Physiology (Bethesda) 29:343-360.